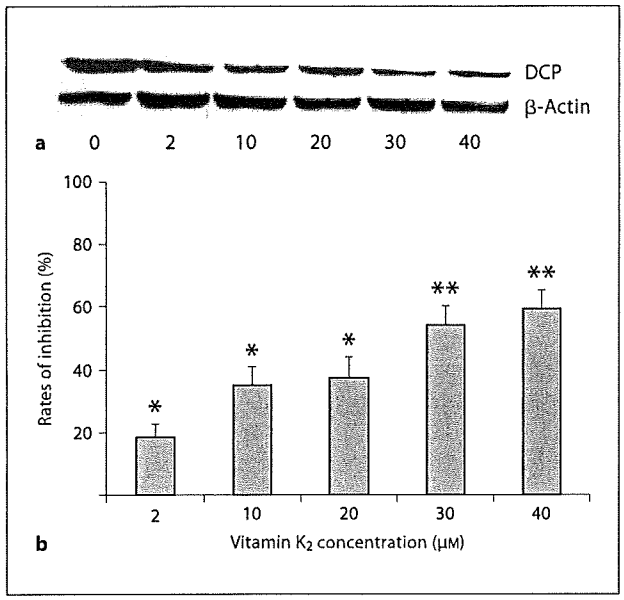

Fig. 5. a Western blot analysis of DCP expression in PLC/PRF/5 cells after treatment with vitamin K_2. Total cell proteins (50 μg) were fractionated through 10% SDS-PAGE, transferred to nitrocellulose filters, and incubated with mice anti-DCP monoclonal antibody. Immunoreactive protein was visualized using an ECL system. **b** The bars are means ± SD (n = 3). The asterisks indicate means that are significantly different when compared to the untreated cells (* $p < 0.05$ and ** $p < 0.01$).

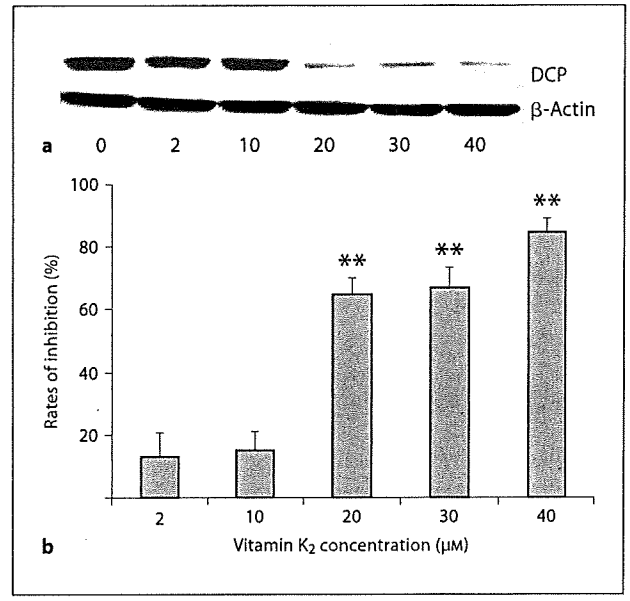

Fig. 6. a Western blot analysis of DCP expression in HepG2 cells. After treatment with vitamin K_2, Western blot analysis was performed as described in figure 5. **b** The bars are means ± SD (n = 3). The asterisks indicate means that are significantly different when compared to the untreated cells (* $p < 0.05$ and ** $p < 0.01$).

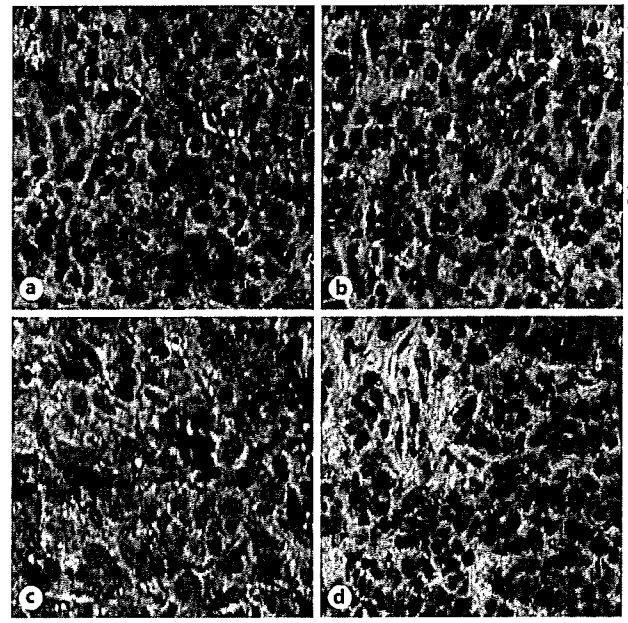

Color version available online

Fig. 7. Immunohistochemical staining of DCP in PLC/PRF/5 (**a, b**) and HepG2 (**c, d**) xenografts. HCC cells were transplanted into nude mice and the mice were orally administered 0 (**a, c**) or 10 mg/kg (**b, d**) of vitamin K_2 for 3 weeks. The sections of xenografts were subjected to immunohistochemistry to detect DCP as described in Materials and Methods. To determine the percentage of positive cells, at least 1,000 cancer cells/slide were counted. Original magnification, ×400.

nist [23]. Reportedly, 44–81% of HCC patients have elevated serum DCP levels [24]. It is hypothesized that as DCP is secreted from HCC cells, it might work as an autologous growth factor for HCC development [8]. Moreover, DCP might also work as a paracrine interaction factor between HCC cells and vascular endothelial cells [7]. Therefore, inhibition of DCP production is considered to be an effective strategy in HCC treatment. Considering the physiological role of vitamin K as a cofactor for γ-glutamyl carboxylase and since vitamin K_2 is a collective reference to compounds composed of menaquinone-n [21], the effects of vitamin K_2 on DCP production and HCC retardation were evaluated. Considering the possible future clinical application, the same correction was found after administration of pharmacological doses of vitamin K_2 to HCC xenografts in mice. Inhibition of HCC growth was observed and vitamin K_2 treatment was well tolerated by animals.

The precise mechanisms of vitamin K_2 treatment are unknown. In this study, we corrected the defect in human hepatoma cell lines in culture and animal models by addition of exogenous vitamin K_2 and a decrease of DCP was observed. Since there was no abnormality in the DNA-encoding prothrombin [5] and since evident cytotoxicity of vitamin K_2 was not observed, vitamin K_2 may maintain the activity of the γ-carboxylase cofactor, vitamin K epoxide reductase and vitamin K reductase (vitamin K cycle) to increase the conversion of DCP to prothrombin [24–26]. During the catalysis in cells, vitamin K_2 may convert from the active form to vitamin K 2,3-epoxide, which must be recycled to the active form by vitamin K epoxide reductase to maintain the coagulation cycle [24–26].

Whatever the mechanisms, the levels of DCP production were decreased and the growth and invasion of HCC cells were inhibited in the presence of vitamin K_2. Therefore, administration of vitamin K_2 should be determined as a promising option for HCC treatment.

Acknowledgements

This project was supported by the National Natural Science Foundation of China, Shandong Provincial Foundation for Natural Science (Y2006C87) and in part by Grants-in-Aid from the Ministry of Education, Science, Sports and Culture of Japan.

References

1 Santamaria E, Munoz J, Fernandez-Irigoven J, Prieto J, Corrales FJ: Toward the discovery of new biomarkers of hepatocellular carcinoma by proteomics. Liver Int 2007;27:163–173.
2 Kim do Y, Paik YH, Ahn SH, Youn YJ, Choi JW, Kim JK, Lee KS, Chon CY, Han KH: PIVKA-II is a useful tumor marker for recurrent hepatocellular carcinoma after surgical resection. Oncology 2007;72(suppl 1):52–57.
3 Hagiwara S, Kudo M, Kawasaki T, Nagashima M, Minami Y, Chung H, Fukunaga T, Kitano M, Nakatani T: Prognostic factors for portal venous invasion in patients with hepatocellular carcinoma. J Gastroenterol 2006; 41:1214–1219.
4 Toyoda H, Kumada T, Kaneoka Y, Osaki Y, Kimura T, Arimoto A, Oka H, Yamazaki O, Manabe T, Urano F, Chung H, Kudo M, Matsunaga T: Prognostic value of pretreatment levels of tumor markers for hepatocellular carcinoma on survival after curative treatment of patients with HCC. J Hepatol 2008; 49:223–232.
5 Naraki T, Kohno N, Saito H, Fujimoto Y, Ohhira M, Morita T, Kohgo Y: Gamma-carboxyglutamic acid content of hepatocellular carcinoma-associated des-gamma-carboxy prothrombin. Biochim Biophys Acta 2002; 1586:287–298.
6 Tamano M, Sugaya H, Oguma M, Lijima M, Yoneda M, Murohisa T, Kojima K, Kuniyoshi T, Majima Y, Hashimoto T, Terano A: Serum and tissue PIVKA-II expression reflect the biological malignant potential of small hepatocellular carcinoma. Hepatol Res 2002; 22:261–269.
7 Fujikawa T, Shiraha H, Ueda N, Takaoka N, Kakanishi Y, Matsuo N, Tanaka S, Nishina S, Suzuki M, Takaki A, Sakaguchi K, Shiratori Y: Des-gamma-carboxyl prothrombin-promoted vascular endothelial cell proliferation and migration. J Biol Chem 2007;282:8741–8748.
8 Suzuki M, Shiraha H, Fujikawa T, Takaoka N, Ueda N, Nakanishi Y, Koike K, Takaki A, Shiratori Y: Des-gamma-carboxy prothrombin is a potential autologous growth factor for hepatocellular carcinoma. J Biol Chem 2005;280:6409–6415.
9 Lawley WJ, Charlton AJ, Hughson AJ, Grundy HH, Brown PM, Jones A: Development of a cell culture/ELISA assay to detect anticoagulant rodenticides and its application to analysis of rodenticide treated grain. J Agric Food Chem 2006;54:1588–1593.
10 Kuwahara N, Higashi T, Nouso K, Ito T, Tsuji T: Immunohistochemical studies of PIVKA-II in hepatocellular carcinoma by indirect immunofluorescence. Acta Med Okayama 1995;49:19–24.
11 Hazra B, Das Sarma M, Kumar B, Basu S, Das K, Pandey BN, Mishra KP: Cytotoxicity of diospyrin and its derivatives in relation to the generation of reactive oxygen species in tumour cells in vitroandin vivo. Chemotherapy 2007;53:173–176.
12 Qu XJ, Yang JL, Russell PJ, Goldstein D: Changes in epidermal growth factor receptor expression in human bladder cancer cell lines following interferon-alpha treatment. J Urol 2004;172:733–738.
13 Franken NA, Rodermond HM, Stap J, Haverman J, van Bree C: Clonogenic assay of cells in vitro. Nat Protoc 2006;1:2315–2319.
14 Wada T, Sata M, Sato J, Tokairin Y, Machiya J, Hirama N, Arao T, Inoue S, Takabatake K, Shibata Y, Kubota I: Clarithromycin suppresses invasiveness of human lung adenocarcinoma cells. Chemotherapy 2007;53:77–84.
15 Okutucu B, Dincer A, Habib O, Zihnioglu F: Comparison of five methods for determination of total plasma protein concentration. J Biochem Biophys Methods 2007;70:709–711.

16 Han MH, Yoo YH, Choi YH: Sanguinarine-induced apoptosis in human leukemia U937 cells via Bcl-2 downregulation and caspase-3 activation. Chemotherapy 2008;54:157–165.
17 Westfall SD, Nilsson EE, Skinner MK: Role of triptolide as an adjunct chemotherapy for ovarian cancer. Chemotherapy 2008;54:67–76.
18 Liu J, Li X, Cheng YN, Cui SX, Chen MH, Xu WF, Tian ZG, Makuuchi M, Tang W, Qu XJ: Inhibition of human gastric carcinoma cell growth by treatment of N(3)-o-toluyl-fluorouracil as a precursor of 5-fluorouracil. Eur J Pharmacol 2007;574:1–7.
19 Ciardiello F, Caputo R, Bianco R, Damiano V, Fontanini G, Cuccato S, De Placido S, Bianco AR, Tortora G: Inhibition of growth factor production and angiogenesis in human cancer cells by ZD1839 (Iressa), a selective epidermal growth factor receptor tyrosine kinase inhibitor. Clin Cancer Res 2001; 7:1459–1465.
20 Ajisaka H, Shimizu K, Miwa K: Immunohistochemical study of protein induced by vitamin K absence or antagonist II in hepatocellular carcinoma. J Surg Oncol 2003;84: 89–93.
21 Otsuka M, Kato N, Shao RX, Hoshida Y, Ijichi H, Koike Y, Taniguchi H, Moriyama M, Shiratori Y, Kawabe T, Omata M: Vitamin K_2 inhibits the growth and invasiveness of hepatocellular carcinoma cells via protein kinase A activation. Hepatology 2004;40:243–251.
22 Uehara S, Gotoh K, Handa H, Tomita H, Senshuu M: Distribution of the heterogeneity of des-gamma-carboxyprothrombin in patients with hepatocellular carcinoma. J Gastroenterol Hepatol 2005;20:1545–1552.
23 Sugimoto H, Takeda S, Inoue S, Kaneko T, Watanabe K, Nakao A: Des-gamma-carboxy prothrombin (DCP) ratio, a novel parameter measured by monoclonal antibodies MU-3 and 19B7, as a new prognostic indicator for hepatocellular carcinoma. Liver Int 2003;23: 38–44.
24 Yuen MF, Lai CL: Serological markers of liver cancer. Best Pract Res Clin Gastroenterol 2005;19:91–99.
25 Wallin R, Sane DC, Hutson SM: Vitamin K 2,3-epoxide reductase and the vitamin K-dependent gamma-carboxylation system. Thromb Res 2002;108:221–226.
26 Otsuka M, Kato N, Ichimura T, Abe S, Tanaka Y, Taniguchi H, Hoshida Y, Moriyama M, Wang Y, Shao RX, Narayan D, Muroyama R, Kanai F, Kawabe T, Isobe T, Omata M: Vitamin K_2 binds 17 β-hydroxysteroid dehydrogenase 4 and modulates estrogen metabolism. Life Sci 2005;76:2473–2482.

Allelic Imbalances and Homozygous Deletion on 8p23.2 for Stepwise Progression of Hepatocarcinogenesis

Yutaka Midorikawa,[1,2,4] Shogo Yamamoto,[1] Shingo Tsuji,[1] Naoko Kamimura,[1] Shumpei Ishikawa,[1] Hisaki Igarashi,[3] Masatoshi Makuuchi,[2] Norihiro Kokudo,[2] Haruhiko Sugimura,[3] and Hiroyuki Aburatani[1]

Early hepatocellular carcinoma (eHCC) originates from the hepatocytes of chronic liver disease and develops into classical hepatocellular carcinoma (HCC). To identify sequential genetic changes in multistep hepatocarcinogenesis, we analyzed molecular karyotypes using oligonucleotide genotyping 50K arrays. First, 1q21.3-44 gain and loss of heterozygosity (LOH) on 1p36.21-36.32 and 17p13.1-13.3 were frequently observed in eHCC, but not in chronic liver diseases, suggesting that such chromosomal aberrations are early, possibly causative events in liver cancer. Next, we detected 25 chromosomal loci associated with liver cancer progression in five HCCs with nodule-in-nodule appearance, in which the inner nodule develops within eHCC lesion. Using these chromosomal regions as independent variables, decision tree analysis was applied on 14 early and 25 overt HCCs, and extracted combination of chromosomal gains on 5q11.1-35.3 and 8q11.1-24.3 and LOH on 4q11-34.3 and 8p11.21-23.3 as distinctive attributes, which can classify early and overt HCCs recursively. In these four altered regions identified as late events of hepatocarcinogenesis, two tumors in 32 overt HCCs analyzed in the present study and one in a set of independent samples of 36 overt HCCs in our previous study harbored a homozygous deletion near the *CSMD1* locus on 8p23.2. *CSMD1* messenger RNA expression was decreased in HCC without 8p23.2 deletion, possibly due to hypermethylation of the CpG islands in its promoter region. *Conclusion:* 1q gain and 1p and 17p LOH are early molecular events, whereas gains in 5q and 8q and LOH on 4q and 8p only occur in advanced HCC, and inactivation of the putative suppressor gene, *CSMD1*, may be the key event in progression of liver cancer. (HEPATOLOGY 2009;49:513-522.)

Abbreviations: cDNA, complementary DNA; eHCC, early hepatocellular carcinoma; FISH, fluorescence in situ hybridization; GIM, genome imbalance map; HCC, hepatocellular carcinoma; HD, homozygous deletion; LOH, loss of heterozygosity; MD, moderately differentiated HCC; mRNA, messenger RNA; NIN, HCC with nodule-in-nodule appearance; PCR, polymerase chain reaction; RT-PCR, reverse-transcription polymerase chain reaction; SNP, single-nucleotide polymorphism; WD, well-differentiated HCC.

From the [1]Division of Genome Science, Research Center for Advanced Science and Technology, and the Division of [2]Hepato-Biliary-Pancreatic Surgery, Department of Surgery, The University of Tokyo, Tokyo, Japan; the [3]1st Department of Pathology, Hamamatsu University School of Medicine, Hamamatsu, Japan; and the [4]Department of Surgery, Teikyo University School of Medicine University Hospital, Mizonokuchi, Kawasaki, Japan.

Received July 1, 2008; accepted October 4, 2008.

Supported in part by Grants-in-Aid for Scientific Research (S) 16101006 and Scientific Research on Priority Areas (C) 17015008 (to H. A.); Grants-in-Aid for Scientific Research (C) 19591601 from The Ministry of Education, Science, Sports, and Culture (to Y. M.) and the Ministry of Health, Labor, and Welfare (19-19); and the Ministry of Education, Culture, Sports, Science and Technology of Japan on Priority Area (20014007) Smoking Research Foundation (to H. S.).

Address reprint requests to: Hiroyuki Aburatani, Genome Science Division, Research Center for Advanced Science and Technology, The University of Tokyo, 4-6-1 Komaba, Meguro-ku, Tokyo 153-8904, Japan. E-mail: haburata-tky@umin.ac.jp; fax: (81)-3-5452-5355.

Published online in Wiley InterScience (www.interscience.wiley.com).

DOI 10.1002/hep.22698

Potential conflict of interest: Nothing to report.

Additional Supporting Information may be found in the online version of this article.

Early hepatocellular carcinoma (eHCC) consists of small hepatocytes with little cellular atypia but with structural atypia. This type of very well-differentiated cancerous tissue is usually characterized by indistinct margins and many portal tracts within the tumor, and it appears to replace the surrounding liver tissue.[1-3] When such small-sized tumors reach 1.5 to 2.0 cm in diameter, less differentiated cancerous tissues arise within the tumor and develop, finally replacing the very well-differentiated hepatocellular carcinoma (HCC). In the course of multistep hepatocarcinogenesis—in which less-differentiated cancerous tissues proliferate with expansive growth within the very well-differentiated liver cancer—the resected tissues frequently exhibit nodule-in-nodule appearance.[1]

HCC with nodule-in-nodule appearance (NIN) is one of the best models for high-throughput genetic investigation currently available, because inner nodules must arise from its background outer nodule, and comparison between the inner and outer nodules provides robust genetic information regarding the progression of liver cancer. Using such samples, we and other groups have identified candidate genes for HCC dedifferentiation using microarray technology.[4-6]

Genome-wide analysis has provided a great deal of information for identification of candidate genes that may be involved in carcinogenesis or cancer progression. Comparative genomic hybridization has been used extensively to detect genome-wide abnormalities, such as copy number changes in various types of cancer, and localization of the regions of many oncogenes and tumor suppressor genes.[7] Recently, array-based comparative genomic hybridization using arrayed genomic DNA or complementary DNA (cDNA) clones,[8,9] or novel algorithms for detecting copy number alterations using single-nucleotide polymorphism (SNP) arrays[10-13] have been developed and applied in various types of cancer research. Previously, we applied a newly developed genome imbalance map (GIM) algorithm,[11] which can detect both genome dosage and allelic imbalance status, to 36 overt HCCs.[14] In this previous study, we demonstrated not only precise chromosomal alterations of HCC but also showed that gene expression profiles reflect chromosomal alterations by integrating the copy number data with the messenger RNA (mRNA) expression intensity.[15]

Using SNP array analysis, Zhao et al.[16] found two homozygous deletions (HDs), 9p23 and 3q25, and high-level amplification within 8q12-13, 12p11, and 22q11 in a large series of lung cancer specimens and cell lines. Identification of amplicons or gain regions may lead to evaluation for likely response to molecular target therapy, such as *EGFR* on 7p12 for gefitinib and erlotinib[17,18] and *ERBB2* on 17q21.1 for trastuzumab.[19] On the other hand, delineation of cancer-specific HDs is biologically significant, because they contain genes responsible for disease, such as *FHIT* on 3p14.2,[20] *GRID2* on 4q22.3,[21] *Parkin* on 6q26,[22] and *WWOX* on 16q23.2.[23] Somatically acquired HD is one of several mutational mechanisms through which both alleles of recessive tumor suppressor genes are inactivated, and searches for additional HD in cancer genomes may yield identification of candidate tumor suppressor genes for carcinogenesis.[20,24]

Decision tree analysis is available for data-mining algorithms to predict the outcome of a disease, such as estimating cancer survivability. Using recursive partitioning, the classification tree-based methodology has identified prognostic factors for stratifying high-risk patients among those with melanoma or breast cancer.[25-27] However, clinical trials have reached their limit of usefulness for predicting the outcomes. In addition, as cancer progresses with accumulation of genetic events and is not the result of a single linear progression due to genetic heterogeneity, comprehensive analysis of molecular events in combination with decision tree analysis would be useful to estimate the prognosis of cancer patients more accurately.[28,29] Chen et al.[30] applied decision tree analysis to microarray data of non–small cell lung cancer and identified five genes as independent predictors of relapse-free and overall survival. On the other hand, tree modeling of comparative genomic hybridization data could provide chromosomal loci as putative prognostic parameters for tumor progression of renal cell carcinoma.[28]

In the present study, we applied GIM using 50K SNP arrays in combination with decision tree analysis using NIN, eHCC, and overt HCC to characterize the regions responsible for initiation of hepatocarcinogenesis and progression of liver cancer (i.e., from chronic liver disease to early stage cancer and to advanced liver cancer). In addition, we observed HD on 8p23.2 frequently in overt HCC and identified a candidate gene for progression of liver cancer within this region.

Patients and Methods

Patients and Tissue Samples. Forty-four patients with HCC undergoing hepatectomy in the Division of Hepato-Biliary-Pancreatic Surgery, Department of Surgery, Graduate School of Medicine, University of Tokyo, were included in this study with informed consent. HCC samples obtained from 44 patients included five NINs (two NINs contained two inner nodules), 14 eHCCs, and 25 overt HCCs. Therefore, we performed GIM analysis using a total of 51 primary tumors and 44 peripheral blood samples. Clinical factors and tumor status based on

histological findings of resected specimens are summarized in Supplementary Table 1.

The surgical specimens were immediately cut into small pieces after resection, snap-frozen in liquid nitrogen, and stored at −80°C.

Cell Culture. Human liver cancer cell lines Hep3B, HepG2, HLE, HT17, Huh6, Huh7, Li-7, and PLC/PRF/5 were obtained and maintained as described.[31]

Genomic DNA Extraction and Oligonucleotide Microarray Analysis. Genomic DNA was isolated from tumor tissues or lymphocyte pellets using a QIAamp DNA Mini Kit (Qiagen, Valencia, CA) in accordance with the manufacturer's protocol. Experimental procedures for GeneChip™ were performed according to the GeneChip Expression Analysis Technical Manual (Affymetrix, Santa Clara, CA) using Human Mapping 50K Array *Xba*I 131 (Affymetrix).

Genome Imbalance Map. The GIM algorithm was applied to raw data of HCC and peripheral blood obtained from SNP arrays. Gene locus information was obtained from the Web sites for Genes On Sequence Map (*Homo sapiens* build 34). The basic concept and method of GIM are described elsewhere.[11]

Decision Tree Analysis. Decision tree analysis can be used to select attributes that are useful to classify the classes of samples in order of the degree of contribution to the classification ability. In this study, class labels were eHCC and overt HCC, and attributes were chromosomal aberrations (1, normal; 2, gain; 3, LOH; 4, uniparental disomy) of each chromosomal locus. Through continued recursive partitioning, the chromosomal aberration loci could be obtained, which could be used to differentiate between eHCC and overt HCC. The integrated data-mining package Orange (http://www.ailab.si/orange/) was used to conduct actual decision tree calculations. The detailed configurations were as follows. Information gain was used as an attribute selection criterion, and to prevent excess partitioning of the tree, prepruning and postpruning procedures were configured.

RNA Extraction, cDNA Synthesis, and Quantitative Reverse-Transcription Polymerase Chain Reaction. Total RNA was isolated from liver cancer cells, HCC, and the background liver as described.[5] Aliquots of 1 μg of purified total RNA were reverse-transcribed into cDNA using SuperScript II (Life Technologies, Palo Alto, CA). Quantitative reverse-transcription polymerase chain reaction (RT-PCR) to detect *CSMD1* gene expression was performed with denaturation at 94°C for 15 seconds, annealing at 62°C for 15 seconds, and extension at 72°C for 30 seconds using Taq Polymerase and 1 μL of cDNA sample. Oligonucleotide primers were designed to amplify cDNA fragments encoding *CSMD1* (148 bp) and *GAPDH* (106 bp) as a control. The primers used were as follows: *CSMD1*, 5′-TCCAGTCATTACCACGGCAC-3′ (forward) and 5′- CATGCCCAGCATAGCCATTG-3′ (reverse); *GAPDH*, 5′- AGCAAGAGCACAAGAGGAAG-3′ (forward) and 5′- GTCTACATGGCAACTGTGAG-3′ (reverse). Quantitative RT-PCR to detect *CSMD1* gene expression was performed using an iCycler (BioRad, Hercules, CA). The relative quantification is given by the ratio between the mean value of the target gene and the mean value of *GAPDH* in each sample.

Table 1. Bisulfite-Modified DNA with CSMD1 Gene-Specific Primers

Primer 1	
Forward	5′-GAGTTATTGTAGGGTTGAGTTGTTT-3′
Reverse	5′-CTCCTCTCCAAATCTCTCCTAACTAC-3′
Primer 2	
Forward	5′-GGAGGTAGTTGGAGAGAGAGTTAG-3′
Reverse	5′-TAAAAATAATTAAATCCAACCTCCAC-3′
Primer 3	
Forward	5′-AGGATTTTGTAATTTTTGTTTTGTT-3′
Reverse	5′-ACAACTCAACCTCTAAACTCACTCTC-3′
Primer 4	
Forward	5′-TTGGGTGATTAAGATTTATTGTTTG-3′
Reverse	5′-CTAAACTTCCCCTCCCTACACTTAC-3′

Fluorescence In Situ Hybridization. Frozen liver cancer and background liver tissues were used for microwave-assisted fluorescence *in situ* hybridization (FISH) analysis as described.[32] Five genomic clones were obtained from a human bacterial artificial chromosome library that contained the following regions: RP11-338C15 for 1q21 (*ATF3*), RP11-335O13 for 1q31-41 (*myogenin*), RP11-462C5 for 1q21, RP11-263K19 for 1q21 (*MUC1*), RP5-973M2 for 1q25.2 (*PTGS2*), and RP11-140K14 for 8p23.2 (*CSMD1*). The FISH signals in carcinoma cells and hepatocytes were scored. Signals were counted manually to exclude those overlapping or those missing the whole nucleus by adjusting the focus.

PCR for Validation of Homozygous Deletion. PCR was performed to validate HD on 8p23.2. DNA fragments of −130 to +29 (primer 1), +26 to +195 (primer 2), and +1793 to +1960 (primer 3) containing HD region in patient 39 were amplified by PCR with *CSMD1* gene-specific primers (Table 1). The sizes of PCR products obtained with primers 1, 2, and 3 were 131, 145, and 148 bp in length, respectively. PCR conditions were as follows: hot start at 95°C for 6 minutes, followed by 35 cycles of 95°C for 30 seconds, 60°C for 30 seconds, and 72°C for 60 seconds, with a final extension at 72°C for 3 minutes. The gene products were electrophoresed on 2% agarose gel.

SNP-Based Loss of Heterozygosity Analysis. LOH analysis at SNP loci (SNP analysis) was performed to validate the allelic status in the chronic liver disease as

described.[14] A search was performed for SNPs on 1p and 17p regions in the National Center for Biotechnology Information SNP database. SNPs within 300 bp were amplified via PCR and genotyped by direct sequencing (Supplementary Table 2). Disappearance of heterozygosity on informative SNPs in the chronic liver disease was considered to be LOH.

5-Aza-2'-Deoxycytidine Treatment. 5-Aza-2'-deoxycytidine (Sigma, St. Louis, MO) was dissolved in phosphate-buffered saline as a 5 mmol/L stock solution and stored in aliquots at −20°C. Three liver cancer cell lines, HepG2, Huh6, and PLC/PRF/5, were split to low density and exposed to 5-Aza-2'-deoxycytidine at a final concentration of 5 μmol/L for 96 hours before harvesting for RNA extraction.

Bisulfite Modification of DNA and Sequencing of Gene Promoter Islands. Aliquots of 2 μg of genomic DNA extracted from liver cancer cells were treated with sodium bisulfite (Sigma, St Louis, MO) and used for bisulfite sequence analysis and methylation-specific polymerase chain reaction, as described.[33] DNA fragments of −130 to +29 (primer 4), +26 to +195 (primer 5), +1793 to +1960 (primer 6), and +2372 to +2659 (primer 7) containing the promoter CpG island were amplified via PCR from bisulfite-modified DNA with *CSMD1* gene-specific primers (Table 2). The sizes of PCR products obtained with primers 1, 2, 3, and 4 were 160, 170, 168, and 288 bp in length, respectively. PCR conditions were as follows: hot start at 95°C for 6 minutes, followed by 35 cycles of 95°C for 30 seconds, 60°C for 30 seconds, and 72°C for 60 seconds, with a final extension at 72°C for 3 minutes. The gene products were cloned into the pGEM-T easy vector (Promega, Madison, WI), and at least 10 colonies were analyzed. Sequencing was performed on an ABI 3100A capillary genetic analyzer, and data were analyzed using Sequencer Version 4.2.2 software.

Bisulfite-modified DNA extracted from liver cancer tissues and from the surrounding normal liver were used for methylation-specific PCR, and amplified with *CSMD1* gene-specific primers:

M-S 5'-TTTTGTTTAGTAGGCGTTGTTTTC-3' and

M-AS 5'-AAATCTTAATCACCCAAACTCGTA-3'

UM-S 5'-GGTTTTGTTTAGTAGGTGTTGTTTT-T-3' and

UM-AS 5'-TAAATCTTAATCACCCAAACTCATA-3'.

The PCR conditions consisted of denaturation of template at 95°C for 6 minutes and successive cycles of 95°C for 30 seconds, 60°C for 30 seconds, and 72°C for 1 minute, with a final extension at 72°C for 3 minutes. Reaction products were separated by electrophoresis on 2% agarose gels, stained with ethidium bromide, and photographed under UV light.

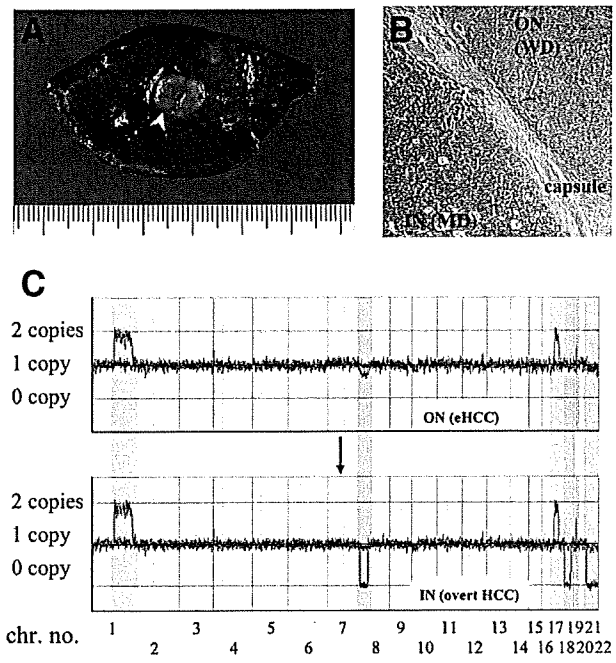

Fig. 1. GIM of a representative NIN sample. (A) Macroscopic findings of HCC with NIN appearance. The outer nodule with indistinct margins (WDHCC) contained an inner nodule with capsule formation, which were diagnosed pathologically as moderately differentiated HCC. Black arrowheads indicate the outer nodule; the white arrowhead indicates the inner nodule. (B) Histological findings of NIN. The outer and inner nodules are conjugated and interposed by the capsule of the inner nodule. IN, inner nodule; MD, moderately differentiated HCC; ON, outer nodule; WD, well-differentiated HCC. (C) Top: Allelic dosage analysis across the whole genome of the outer nodule (eHCC) in patient 5. As indicated with a green box, GIM showed gains of 1q21.2-qter and 17q21.32-qter in the outer nodule of this patient. Bottom: Allelic dosage analysis of inner nodule (overt HCC) of the same patient. In addition to gains of 1q21.2-qter and 17q21.32-qter, LOH of 8p32.2-11.21, 18q12.3-22.1, chromosome 21, and chromosome 22 (indicated by yellow box), were found only in the inner nodule on GIM analysis.

Results

A Gain on 1q and LOH on 1p and 17p as Early Event in Hepatocarcinogenesis. The GIM was applied to 51 HCC nodules in 44 patients, comparing their copy numbers to those of peripheral blood (Fig. 1). Using a 50K *Xba*I SNP array, the mean call rates, in which SNP array discriminate genotypes of DNA sequences, were 98.8 ± 0.7% in HCC and 99.0 ± 0.7% in controls, and the mean rates of informative heterozygous calls were 24.9 ± 2.1% in HCC and 26.5 ± 0.7% in controls.

Regenerative nodular lesions in the cirrhotic liver are considered to have precancerous potential. GIM analysis revealed a gain on 1q21.3-44 (63%) and LOH on 1p36.21-36.32 (36%) and 17p13.1-13.3 (42%) fre-

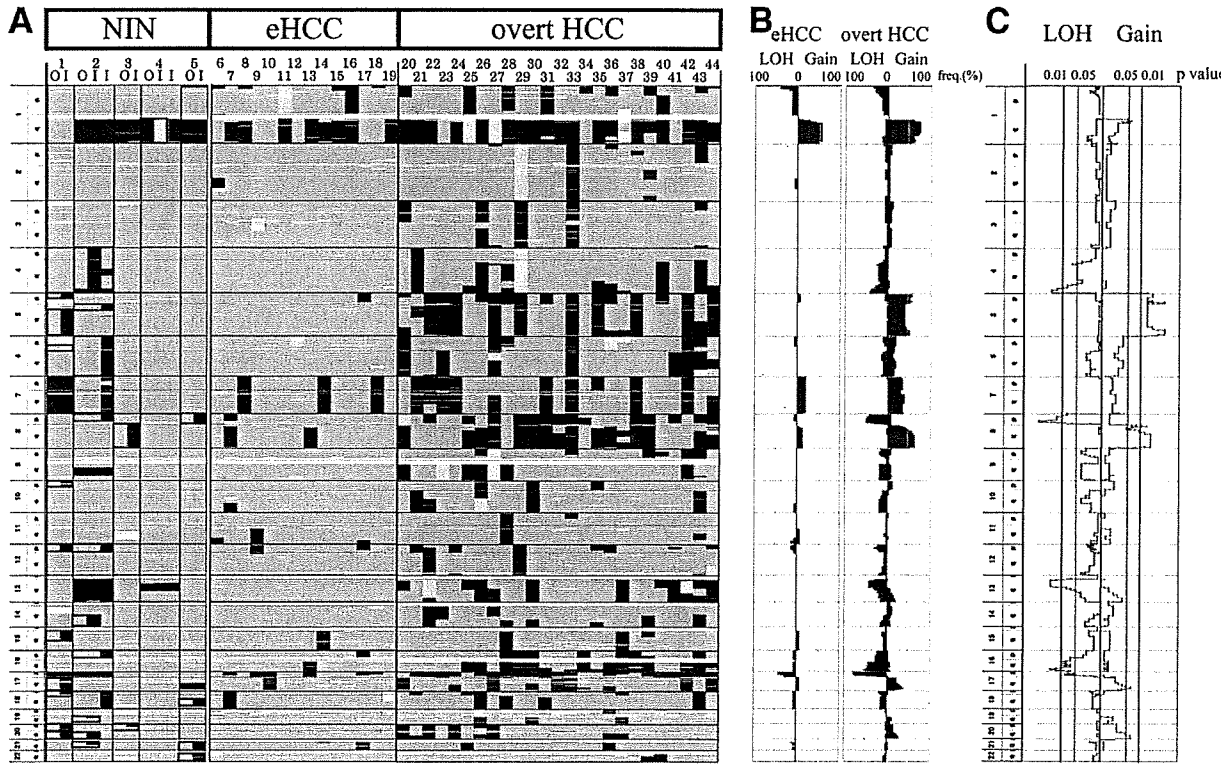

Fig. 2. Overview of genome imbalance regions in HCC. (A) Case numbers are indicated on the top row and chromosome site bands are shown on the vertical column. In the genetic alteration status group, the symbols indicate the following: red box, informative case for gain; blue box, LOH; yellow box, uniparental disomy or UPT; gray box, retention; white box, not informative. Regions with genetic alterations between inner and outer nodules in NIN are surrounded with a solid line and summarized in Supplementary Table 2. (B) Frequency of copy number alterations and LOH in 14 eHCC and 25 overt HCC samples. (C) *P* values by Fisher's exact test between early and overt HCC. Some chromosomal regions showed consistent relationships with tumor progression; for example, chromosomal gains on 5p, 5q, 8q, 17q24.2-24.3, and 20q13.12-qter and LOH on 4q31.3-qter, 8p, 13qcen-21.31, 16pcen-11.2, 16q, and 17p were significantly associated with overt HCC, as compared to eHCC. eHCC, early hepatocellular carcinoma; I, inner nodule; LOH, loss of heterozygosity; NIN, nodule-in-nodule appearance; O, outer nodule.

quently even in five outer nodules in NIN and 14 eHCCs (Fig. 2). To determine whether chromosomal aberrations on 1q, 1p, and 17p in eHCC already occurred in the background liver, we evaluated allelic status using FISH analysis on 1q and SNP-based LOH analysis on 1p and 17p for all the cancerous tissue and the surrounding noncancerous liver tissue (Fig. 3). These analyses confirmed that the allelic status of cancerous tissue on 1q gain (Fig. 3B) and LOH on 1p and 17p (Fig. 3D) corresponded with GIM data. On the other hand, we found no chromosomal alterations on 1q (Fig. 3C) and 17p (Fig. 3D), and only one case of 1p LOH in the background liver tissue.

Based on these results, we concluded that a gain on chromosome 1q and LOH on chromosome 1p and 17p, which were identified using GIM analysis, are the initial events in hepatocarcinogenesis and do not occur in the background liver, and that these regions may contain candidate genes responsible for initiation of hepatocarcinogenesis.

Genome Imbalance Regions in Progression of HCC. To identify stepwise chromosomal aberrations in progression of liver cancer, we compared chromosomal alterations of the outer nodule to those of the inner nodule in NIN samples (Fig. 1C). All the chromosomal alterations found in the outer nodules were also observed in the corresponding inner nodules, suggesting that the latter had arisen from the former (Fig. 2A). GIM analysis identified chromosomal gains on 15 and LOH on 10 loci between the five outer and seven inner nodules (Fig. 2A; Supplementary Table 3). Using these chromosomal loci identified in NIN as independent variables, we performed decision tree analysis with regard to 14 eHCCs and 25 overt HCCs (Supplementary Fig. 1). Decision tree analysis extracted combinations of chromosomal aberrations on 5q11.1-35.3, 8q11.1-24.3, 4q11-34.3, and 8p11.21-23.3 in progression as distinctive attributes, which can classify early and overt HCCs recursively (Fig. 4A). Estimating the chromosomal aberrations by decision tree analysis with regard to progression of HCC, classification

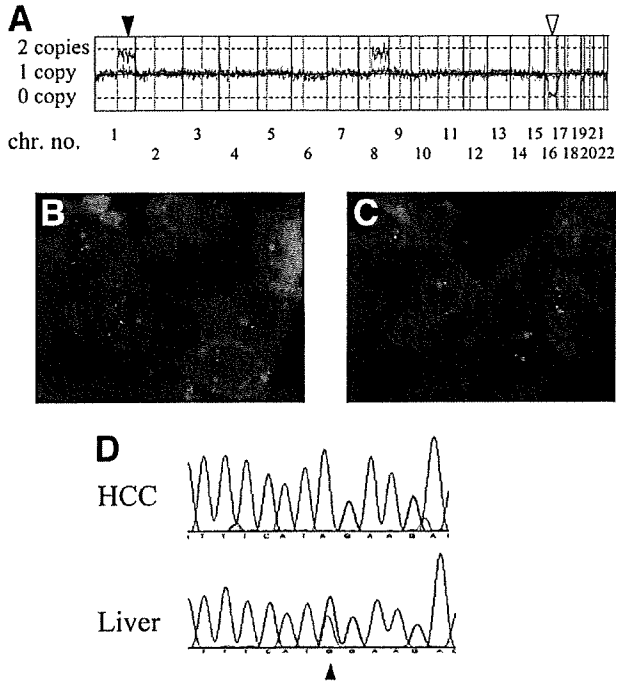

Fig. 3. Validation of allelic imbalance of patient 13 (eHCC). (A) GIM showing gains of 1q and 8q and LOH of 16q and 17p arms. The black arrowhead indicates the position of the bac clone (RP11-462C5 for 1q21); the white arrowhead indicates the position of the SNP loci (rs10491091 for 17p13.1). (B,C) Fluorescence *in situ* hybridization analysis demonstrated three distinct signals representing 1q21 in liver cancer cells (B), but two pairs in the corresponding background liver (C). Green, RP11-338C15 (1q21, *ATF3*); orange, CEP1. (D) SNP-based LOH analysis using direct sequencing at rs10491091 (A/G) showed LOH of the 17p arm in HCC but retention of heterozygosity of the 17p arm in the background liver obtained from the same patient (arrowhead, rs10491091).

accuracy between early and overt HCC was 86.8% by five-fold cross-validation.

This method was applied to our previous study for a set of independent samples of 36 overt HCCs using 10K array, and 32 cases (89%) were classified as overt HCC (Fig. 4B).

These results suggest that gains on 5q11.1-35.3 and 8q11.1-24.3 and LOH on 4q11-34.3 and 8p11.21-23.3 only occur in progression with dedifferentiation from early to advanced liver cancer.

Homozygous Deletion Within Chromosome Segments 8p23.2. The results of our previous study using GIM analysis with a 10K array indicated HD within 8p23.2-23.3.[14] The results of the present study also indicated HD within 8p23.2 in two patients in seven inner nodules and 25 overt HCCs, but in neither five outer nodules nor 14 eHCCs, and therefore HD within this region was identified in 2 of 32 classical HCCs (6%). The lengths of the HD regions were 2,446 kb and 126 kb in 8p23.2-23.3 near the *CSMD1* gene alone (Fig. 5A), which were validated using FISH analysis for patient 2 (Fig. 5B) or PCR analysis for patient 39 (Fig. 5C) and prompted an investigation of the inactivation of this gene in the progression of liver cancer.

Methylation of the Promoter Is Inversely Correlated with CSMD1 Gene Expression. First, we investigated *CSMD1* mRNA expression levels via RT-PCR analysis performed on eight liver cancer cell lines and normal liver tissues obtained from patients with liver metastasis from colorectal cancer as controls. The results of RT-PCR indicated that *CSMD1* mRNA levels were

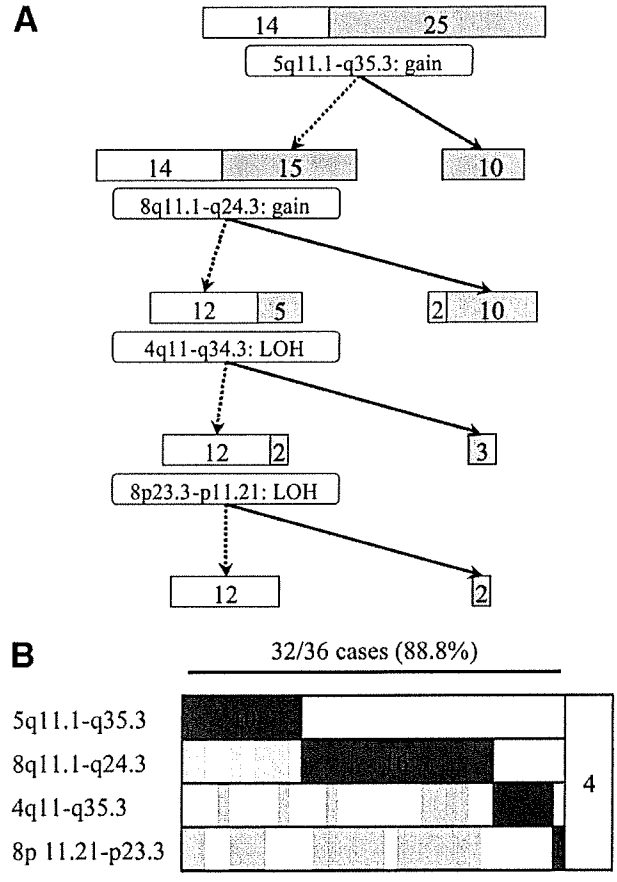

Fig. 4. Decision tree analysis for classification of early and overt HCC. (A) All 38 samples (14 eHCCs and 25 overt HCCs) were used as the initial dataset. As recursive partitioning proceeds through extracting the overt HCCs enriched group, all of the selected features have independently significant roles characterizing the differences between eHCCs and overt HCCs. For instance, in the first portioning of samples, 10 overt HCC samples are extracted from 14 eHCC and 25 overt HCC samples caused by the chromosomal gain of 5q11.1-35.3. The number of samples of eHCC and overt HCC in each split are indicated in white and gray boxes, respectively. Solid line, with alteration; dashed line, without alteration. (B) Thirty-two (89%) of 36 independent overt HCC samples using 10K array in our previous study harbored no fewer than one chromosomal aberration among four regions extracted by decision tree analysis. The columns and rows represent the tissue samples and chromosomal regions, respectively. Chromosomal gains in each region are shown in red, and LOH is shown in blue.

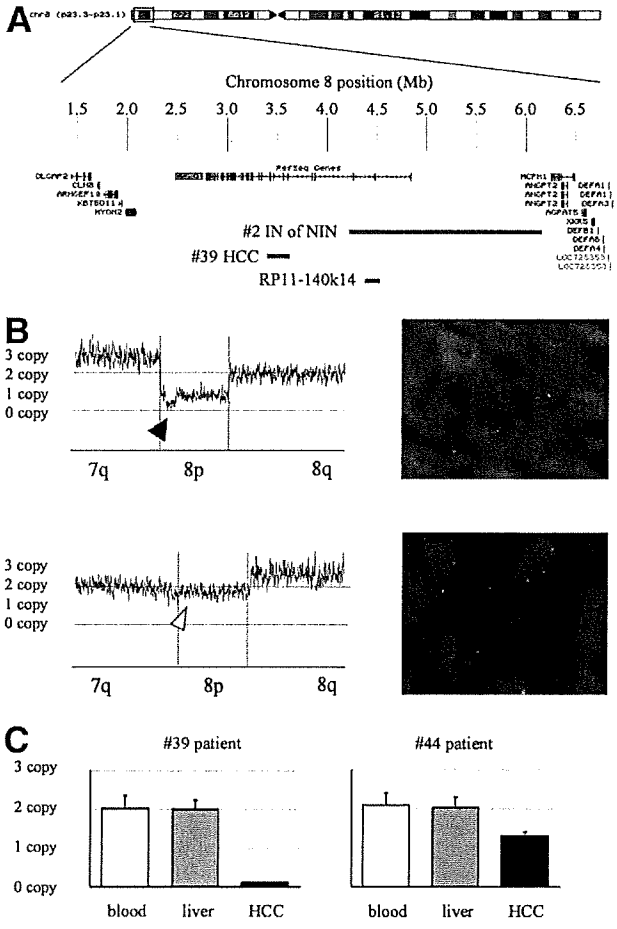

Fig. 5. *CSMD1* gene near homozygously deleted region at 8p23.2-23.3. (A) HD region in two advanced liver cancers containing the *CSMD1* gene. The blue line shows the region with HD in each sample, and the black line represents the location of the bac clone, RP11-140K14, used for FISH. (B) Validation of HD on 8p23.2 via FISH analysis in liver cancer. Top: FISH revealed no signals of the *CSMD1* locus, but only of the centromere of chromosome 8 in the inner nodule of patient 2 with HD on 8p23.2 via GIM analysis (black arrowhead). Bottom: FISH revealed two pairs of signals of the *CSMD1* locus and the centromere of chromosome 8 in patient 35 with retention of heterozygosity on 8p23.2 (white arrowhead). Orange, RP11-140K14 (8p23.2, *CSMD1*); green, CEP8. IN, inner nodule; NIN, nodule-in-nodule appearance. (C) Validation of HD on 8p23.2 via PCR analysis in liver cancer. In HCC of patient 39, PCR products were not observed in any loci indicated as HD regions by GIM, but all the products were detectable in the background liver and blood of the same patient. On the other hand, in patient 44, whose HCC samples harbored LOH in 8p23.2, PCR analysis revealed a decrease of about 50% in expression intensity in HCC compared with the background liver and blood samples. ΦX174 DNA-*Hae*III digest was used as a size marker.

much lower in Hep3B, HepG2, Huh6, Huh7, and Li-7 as compared with the normal liver, whereas the level of *CSMD1* transcript was not decreased in HLE, HT17, or PLC/PRF/5 (Fig. 6A).

Using sequence-tagged site markers, we analyzed the allelic status of eight liver cancer cell lines, none of which had homozygous deletions near the *CSMD1* locus within 8p23.2 (Supplementary Fig. 2). To determine whether epigenetic silencing by promoter methylation could account for the low expression levels of *CSMD1*, we investigated the methylation levels of the promoter region of the *CSMD1* gene in four liver cancer cell lines: HepG2, Huh6, HT17, and PLC/PRF/5. The sites analyzed for methylation status are shown in Supplementary Fig. 3.

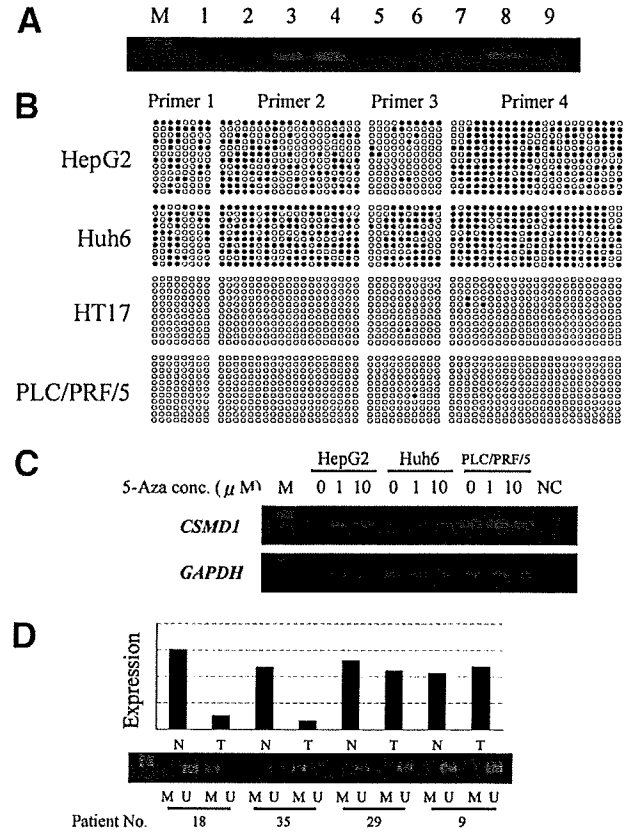

Fig. 6. Epigenetic regulation of *CSMD1* gene expression. (A) Expression of *CSMD1* mRNA in hepatoma cells. RT-PCR analysis of the *CSMD1* mRNA levels in hepatoma cell lines. Lane 1, Hep3B; lane 2, HepG2; lane 3, HLE; lane 4, HT17; lane 5, Huh6; lane 6, Huh7; lane 7, Li-7; lane 8, PLC/PRF/5; lane 9, blank; M, ΦX174 DNA-*Hae* III digest (marker). (B) Methylation status of the *CSMD1* promoter region by bisulfite sequence analysis in Hep3B, HepG2, Huh6, Li-7, HT-17, and PLC/PRF/5 cells. Each CpG dinucleotide within the amplicon is represented by a column and each sequenced clone is represented by a row. Open circles indicate that the cytosine residue of the dinucleotide was unmethylated, while closed circles indicate that it was unmethylated. (C) Expression of *CSMD1* mRNA in hepatoma cells after inhibition of *DNMT* with 5-Aza-2'-deoxycytidine. Numbers at the top of the figure indicate the concentration of 5-Aza-2'-deoxycytidine. NC, negative control. (D) Methylation status of the promoter region of the *CSMD1* gene by methylation-specific PCR, and analysis of *CSMD1* gene expression of representative samples. Patients 18 and 35, in whom CSMD1 mRNA expression was decreased, showed heavy methylation in the promoter region, whereas no methylation was observed in those without down-regulation of CSMD1 expression. Sample numbers 18, 35, and 29 were overt HCCs, and 9 was eHCC. M, methylated; U, unmethylated; T, HCC; N, background liver. ΦX174 DNA-*Hae*III digest was used as a size marker.

Bisulfite genomic sequencing analysis indicated no methylation in PLC/PRF/5 or HT17cells, in which the mRNA expression levels are high, whereas the methylation levels were 42.2% and 84.0% in HepG2 and Huh6, respectively, with low *CSMD1* expression levels (Fig. 6B).

Next, to further explore the possibility that the *CSMD1* gene may be a target for epigenetic silencing in liver cancer, we analyzed a panel of cultured liver cancer cell lines for *CSMD1* expression. Cells were cultured in the presence or absence of the DNA demethylating drug 5-Aza-2'-deoxycytidine, and total RNA was harvested. cDNA was then synthesized from total RNA, and RT-PCR was performed to determine expression of *CSMD1*. Transcript abundance in HepG2 and Huh6 cells with very low *CSMD1* expression levels was markedly increased following culture in the presence of 5-Aza-2'-deoxycytidine. In contrast, PLC/PRF/5 showed high levels of *CSMD1* expression, and the relative abundance of this transcript was not altered by culture in the presence of 5-Aza-2'-deoxycytidine (Fig. 6C).

Furthermore, methylation-specific PCR was performed with regard to 14 eHCCs, 25 overt HCCs, and the corresponding liver tissue, in which *CSMD1* mRNA expression was determined via quantitative RT-PCR analysis. The results of quantitative RT-PCR analysis indicated that *CSMD1* expression was decreased to less than half in seven of 25 overt HCCs in comparison with the background liver, whereas *CSMD1* mRNA was not altered in any eHCC sample examined. Using methylation-specific PCR analysis, seven tumors with lower *CSMD1* mRNA level were shown to harbor heavy methylation of CpG islands of the *CSMD1* gene—that is, *CSMD1* expression level was correlated with the methylation status in its promoter region (Fig. 6D).

Taken together, these observations suggest that *CSMD1* mRNA expression levels are suppressed by heavy methylation of the CpG island surrounding the first exon in the progression of liver cancer.

Discussion

In the course of liver cancer progression, well-differentiated HCC (WD) dedifferentiates into moderately differentiated HCC (MD), so-called classical HCC. Clinical observations often indicate that treated WD with capsule formation and distinct margin recurs, as in the case of MD, even after curative resection. In addition to the observation that about 20% of small HCCs of distinctly nodular type are uniformly composed of well-differentiated cancerous tissue,[34] such WD should be treated as overt HCC.[35]

On the other hand, Takayama et al.[3] reported that eHCC, which is well differentiated, is a distinct clinical entity with a high surgical cure rate, as compared to overt HCC.[3] Along with macroscopic and histological features, eHCC should be distinguished from overt HCC, including WDHCC with distinct margins. Previously, we reported allelic imbalance status of HCC, in which all WDHCC samples analyzed by 10K SNP array in our previous study had distinct margins.[14] In the present study, we focused on eHCC in the initiation of hepatocarcinogenesis for analysis of allelic changes.

Although there is very little cellular atypia in eHCC, our results indicate that all cases of eHCC have genomic alterations. Especially, 1q21.3-44 gain and LOH on 1p36.21-36.32 and 17p13.1-13.3 were observed frequently in eHCC, whereas all the background liver tissue—with the exception of one case with the 1p arm—showed no alterations in these regions on FISH and SNP-based LOH analysis. No chromosomal aberrations in the background liver on 1q and 17p in the present study is consistent with previous reports that in the cirrhotic liver or dysplastic nodules, allelic alterations on 1q and 17p arms are rare.[36-38] On the other hand, 1p, 3p (*TGFB2R*), 4q, 6q (*IGF2R*), 8p, 13q (*RB*), 16q (*CDH1*), and 22q arms sometimes harbor genomic changes,[37,39-45] but our data showed that 1p LOH of the cirrhotic liver was very rare (2%), and we assumed that chromosomal changes in 1q, 1p, and 17p are of clinical importance in initiation of hepatocarcinogenesis.

We used NIN in this study as a model of tumor progression. By comparison of the inner and outer nodules of NIN samples, we identified the sequential chromosomal alterations accompanied with dedifferentiation of liver cancer. To generalize such chromosomal aberrations, we used recursive partitioning analysis to create a decision tree and succeeded in narrowing the chromosomal loci responsible for liver cancer progression with high classification accuracy (i.e., gains on 5q11.1-35.3 and 8q11.1-24.3 and LOH on 4q11-34.3 and 8p11.21-23.3). In addition to these four chromosomal aberrations identified by decision tree analysis, Fisher's exact test revealed six chromosomal loci with a significant difference between eHCC and overt HCC ($P < 0.05$). However, univariate analysis cannot detect the relationship between the chromosomal aberrations,[25] and we found that four chromosomal aberrations on 5q, 8q, 4q, and 8p occurred independently ($P < 0.0001$ [χ^2 test]), reflecting a high degree of genetic heterogeneity in liver cancer progression.[28] Furthermore, these four regions were applied to the independent set of overt HCCs in our previous study using the 10K array,[14] and 32 tumors (89%) in 36 overt HCCs were recognized as advanced liver cancer, indicating that gains on 5q and 8q and LOH on 4q and 8p occur

in accordance with liver cancer progression from the early stages of HCC with high frequency.

Genes that are targets for HD in cancer are often subject to tumor suppressor genes. The GIM allowed us to identify recurrent HD on 8p23.2 in three of 68 overt HCCs (one of 36 cases in our previous report using a 10K array[14] and two of 32 tumors in the present study using a 50K *Xba*I array), not in any eHCCs. HD detected by GIM using a 10K array indicated six candidate genes near 8p23.2-23.3. On the other hand, analysis of a novel homozygously deleted region at 8p23.2 in advanced HCC specified *CSMD1*, the deletion of which has been reported in head and neck cancer,[46] as a gene of potential interest in liver cancer progression in the present study using a 50K *Xba*I array, possibly due to higher resolution.

CSMD1 is one of the largest genes, the genomic sequence of which is more than 2.0 Mb, and contains multiple CUB and sushi domains.[46] *CSMD1* is considered a putative suppressor gene because of the presence of multiple regions of HD at the *CSMD1* locus and epigenetic inactivation in head and neck squamous cell carcinoma.[47,48] Expression analysis by CodeLink revealed that the *CSMD1* gene mRNA levels were as high as those of other tumor suppressor genes in the liver, which prompted analysis of the mechanism of inactivation of this gene (Supplementary Fig. 4). As in previous reports, we found that in addition to HD, *CSMD1* mRNA expression was decreased due to heavy methylation of the promoter region, the CpG islands around the first exon, suggesting that *CSMD1* functions as a tumor suppressor from early to advanced liver cancer.

In conclusion, we applied GIM analysis for NIN, eHCC, and overt HCC, and recursive partitioning analysis elucidated the chromosomal alterations involved in initiation of hepatocarcinogenesis and progression of liver cancer. Furthermore, we found HD frequently on 8p23.2, and mRNA expression of the extremely large gene *CSMD1* within this region was decreased in overt HCC, suggesting that *CSMD1* plays a pivotal role in liver cancer progression.

Acknowledgment: We thank Hiroko Meguro, Takayuki Isagawa, and Kiyoko Nagura for valuable technical assistance.

References

1. Kojiro M. 'Nodule-in-nodule' appearance in hepatocellular carcinoma: its significance as a morphologic marker of dedifferentiation. Intervirology 2004;47:179-183.
2. Sakamoto M, Hirohashi S, Shimosato Y. Early stages of multistep hepatocarcinogenesis: adenomatous hyperplasia and early hepatocellular carcinoma. Hum Pathol 1991;22:172-178.
3. Takayama T, Makuuchi M, Hirohashi S, Sakamoto M, Yamamoto J, Shimada, et al. Early hepatocellular carcinoma as an entity with a high rate of surgical cure. HEPATOLOGY 1998;28:1241-1246.
4. Nam SW, Lee JH, Noh JH, Lee SN, Kim SY, Lee SH, et al. Comparative analysis of expression profiling of early-stage carcinogenesis using nodule-in-nodule-type hepatocellular carcinoma. Eur J Gastroenterol Hepatol 2006;18:239-247.
5. Midorikawa Y, Tsutsumi S, Taniguchi H, Ishii M, Kobune Y, Kodama T, et al. Identification of genes associated with dedifferentiation of hepatocellular carcinoma with expression profiling analysis. Jpn J Cancer Res 2002; 93:636-643.
6. Chuma M, Sakamoto M, Yamazaki K, Ohta T, Ohki M, Asaka M, et al. Expression profiling in multistage hepatocarcinogenesis: identification of HSP70 as a molecular marker of early hepatocellular carcinoma. HEPATOLOGY 2003;37:198-207.
7. Kallioniemi A, Kallioniemi OP, Sudar D, Rutovitz D, Gray JW, Waldman F, et al. Comparative genomic hybridization for molecular cytogenetic analysis of solid tumors. Science 1992;258:818-821.
8. Pinkel D, Segraves R, Sudar D, Clark S, Poole I, Kowbel D, et al. High resolution analysis of DNA copy number variation using comparative genomic hybridization to microarrays. Nat Genet 1998;20:207-211.
9. Pollack JR, Sorlie T, Perou CM, Rees CA, Jeffrey SS, Lonning PE, et al. Microarray analysis reveals a major direct role of DNA copy number alteration in the transcriptional program of human breast tumors. Proc Natl Acad Sci U S A 2002;99:12963-12968.
10. Bignell GR, Huang J, Greshock J, Watt S, Butler A, West S, et al. High-resolution analysis of DNA copy number using oligonucleotide microarrays. Genome Res 2004;14:287-295.
11. Ishikawa S, Komura D, Tsuji S, Nishimura K, Yamamoto S, Panda B, et al. Allelic dosage analysis with genotyping microarrays. Biochem Biophys Res Commun 2005;333:1309-1314.
12. Nannya Y, Sanada M, Nakazaki K, Hosoya N, Wang L, Hangaishi A, et al. A robust algorithm for copy number detection using high-density oligonucleotide single nucleotide polymorphism genotyping arrays. Cancer Res 2005;65:6071-6079.
13. Zhao X, Li C, Paez JG, Chin K, Janne PA, Chen TH, et al. An integrated view of copy number and allelic alterations in the cancer genome using single nucleotide polymorphism arrays. Cancer Res 2004;64:3060-3071.
14. Midorikawa Y, Yamamoto S, Ishikawa S, Kamimura N, Igarashi H, Sugimura H, et al. Molecular karyotyping of human hepatocellular carcinoma using single-nucleotide polymorphism arrays. Oncogene 2006;25:5581-5590.
15. Midorikawa Y, Tsutsumi S, Nishimura K, Kamimura N, Kano M, Sakamoto H, et al. Distinct chromosomal bias of gene expression signatures in the progression of hepatocellular carcinoma. Cancer Res 2004;64:7263-7270.
16. Zhao X, Weir BA, LaFramboise T, Lin M, Beroukhim R, Garraway L, et al. Homozygous deletions and chromosome amplifications in human lung carcinomas revealed by single nucleotide polymorphism array analysis. Cancer Res 2005;65:5561-5570.
17. Tsao MS, Sakurada A, Cutz JC, Zhu CQ, Kamel-Reid S, Squire J, et al. Erlotinib in lung cancer—molecular and clinical predictors of outcome. N Engl J Med 2005;353:133-144.
18. Hirsch FR, Varella-Garcia M, McCoy J, West H, Xavier AC, Gumerlock P, et al. Increased epidermal growth factor receptor gene copy number detected by fluorescence in situ hybridization associates with increased sensitivity to gefitinib in patients with bronchioloalveolar carcinoma subtypes: a Southwest Oncology Group Study. J Clin Oncol 2005;23:6838-6845.
19. Seidman AD, Fornier MN, Esteva FJ, Tan L, Kaptain S, Bach A, et al. Weekly trastuzumab and paclitaxel therapy for metastatic breast cancer with analysis of efficacy by HER2 immunophenotype and gene amplification. J Clin Oncol 2001;19:2587-2595.
20. Ohta M, Inoue H, Cotticelli MG, Kastury K, Baffa R, Palazzo J, et al. The FHIT gene, spanning the chromosome 3p14.2 fragile site and renal carcinoma-associated t(3;8) breakpoint, is abnormal in digestive tract cancers. Cell 1996;84:587-597.

21. Rozier L, El-Achkar E, Apiou F, Debatisse M. Characterization of a conserved aphidicolin-sensitive common fragile site at human 4q22 and mouse 6C1: possible association with an inherited disease and cancer. Oncogene 2004;23:6872-6880.
22. Cesari R, Martin ES, Calin GA, Pentimalli F, Bichi R, McAdams H, et al. Parkin, a gene implicated in autosomal recessive juvenile parkinsonism, is a candidate tumor suppressor gene on chromosome 6q25–q27. Proc Natl Acad Sci U S A 2003;100:5956-5961.
23. Bednarek AK, Keck-Waggoner CL, Daniel RL, Laflin KJ, Bergsagel PL, Kiguchi K, et al. WWOX, the FRA16D gene, behaves as a suppressor of tumor growth. Cancer Res 2001;61:8068-8073.
24. Bednarek AK, Laflin KJ, Daniel RL, Liao Q, Hawkins KA, Aldaz CM. WWOX, a novel WW domain-containing protein mapping to human chromosome 16q23.3-24.1, a region frequently affected in breast cancer. Cancer Res 2000;60:2140-2145.
25. Freedman GM, Hanlon AL, Fowble BL, Anderson PR, Nicolaou N. Recursive partitioning identifies patients at high and low risk for ipsilateral tumor recurrence after breast-conserving surgery and radiation. J Clin Oncol 2002;20:4015-4021.
26. Gimotty PA, Elder DE, Fraker DL, Botbyl J, Sellers K, Elenitsas R, et al. Identification of high-risk patients among those diagnosed with thin cutaneous melanomas. J Clin Oncol 2007;25:1129-1134.
27. Delen D, Walker G, Kadam A. Predicting breast cancer survivability: a comparison of three data mining methods. Artif Intell Med 2005;34:113-127.
28. Jiang F, Desper R, Papadimitriou CH, Schaffer AA, Kallioniemi OP, Richter J, et al. Construction of evolutionary tree models for renal cell carcinoma from comparative genomic hybridization data. Cancer Res 2000;60:6503-6509.
29. Desper R, Jiang F, Kallioniemi OP, Moch H, Papadimitriou CH, Schaffer AA. Distance-based reconstruction of tree models for oncogenesis. J Comput Biol 2000;7:789-803.
30. Chen HY, Yu SL, Chen CH, Chang GC, Chen CY, Yuan A, et al. A five-gene signature and clinical outcome in non-small-cell lung cancer. N Engl J Med 2007;356:11-20.
31. Midorikawa Y, Ishikawa S, Iwanari H, Imamura T, Sakamoto H, Miyazono K, et al. Glypican-3, overexpressed in hepatocellular carcinoma, modulates FGF2 and BMP-7 signaling. Int J Cancer 2003;103:455-465.
32. Kitayama Y, Igarashi H, Watanabe F, Maruyama Y, Kanamori M, Sugimura H. Nonrandom chromosomal numerical abnormality predicting prognosis of gastric cancer: a retrospective study of 51 cases using pathology archives. Lab Invest 2003;83:1311-1320.
33. Herman JG, Graff JR, Myohanen S, Nelkin BD, Baylin SB. Methylation-specific PCR: a novel PCR assay for methylation status of CpG islands. Proc Natl Acad Sci U S A 1996;93:9821-9826.
34. Kojiro M. Focus on dysplastic nodules and early hepatocellular carcinoma: an Eastern point of view. Liver Transpl 2004;10:S3-S8.
35. Japan Liver Cancer Society Group. General rules for the clinical and pathological study of primary liver cancer: 2nd ed. Tokyo: Kanchura; 2003:15-16.
36. Nishida N, Fukuda Y, Kokuryu H, Sadamoto T, Isowa G, Honda K, et al. Accumulation of allelic loss on arms of chromosomes 13q, 16q and 17p in the advanced stages of human hepatocellular carcinoma. Int J Cancer 1992;51:862-868.
37. Ho MK, Lee JM, Chan CK, Ng IO. Allelic alterations in nontumorous liver tissues and corresponding hepatocellular carcinomas from chinese patients. Hum Pathol 2003;34:699-705.
38. Wong N, Lai P, Lee SW, Fan S, Pang E, Liew CT, et al. Assessment of genetic changes in hepatocellular carcinoma by comparative genomic hybridization analysis: relationship to disease stage, tumor size, and cirrhosis. Am J Pathol 1999;154:37-43.
39. Ashida K, Kishimoto Y, Nakamoto K, Wada K, Shiota G, Hirooka Y, et al. Loss of heterozygosity of the retinoblastoma gene in liver cirrhosis accompanying hepatocellular carcinoma. J Cancer Res Clin Oncol 1997;123:489-495.
40. Kanai Y, Ushijima S, Tsuda H, Sakamoto M, Hirohashi S. Aberrant DNA methylation precedes loss of heterozygosity on chromosome 16 in chronic hepatitis and liver cirrhosis. Cancer Lett 2000;148:73-80.
41. Maggioni M, Coggi G, Cassani B, Bianchi P, Romagnoli S, Mandelli A, et al. Molecular changes in hepatocellular dysplastic nodules on microdissected liver biopsies. HEPATOLOGY 2000;32:942-946.
42. Roncalli M, Bianchi P, Grimaldi GC, Ricci D, Laghi L, Maggioni M, et al. Fractional allelic loss in non-end-stage cirrhosis: correlations with hepatocellular carcinoma development during follow-up. HEPATOLOGY 2000;31:846-850.
43. Nagai H, Terada Y, Tajiri T, Yabe A, Onda M, Nagahata T, et al. Characterization of liver-cirrhosis nodules by analysis of gene-expression profiles and patterns of allelic loss. J Hum Genet 2004;49:246-255.
44. Yamada T, De Souza AT, Finkelstein S, Jirtle RL. Loss of the gene encoding mannose 6-phosphate/insulin-like growth factor II receptor is an early event in liver carcinogenesis. Proc Natl Acad Sci U S A 1997;94:10351-10355.
45. Sun M, Eshleman JR, Ferrell LD, Jacobs G, Sudilovsky EC, Tuthill R, et al. An early lesion in hepatic carcinogenesis: loss of heterozygosity in human cirrhotic livers and dysplastic nodules at the 1p36–p34 region. HEPATOLOGY 2001;33:1415-1424.
46. Sun PC, Uppaluri R, Schmidt AP, Pashia ME, Quant EC, Sunwoo JB, et al. Transcript map of the 8p23 putative tumor suppressor region. Genomics 2001;75:17-25.
47. Toomes C, Jackson A, Maguire K, Wood J, Gollin S, Ishwad C, et al. The presence of multiple regions of homozygous deletion at the CSMD1 locus in oral squamous cell carcinoma question the role of CSMD1 in head and neck carcinogenesis. Genes Chromosomes Cancer 2003;37:132-140.
48. Richter TM, Tong BD, Scholnick SB. Epigenetic inactivation and aberrant transcription of CSMD1 in squamous cell carcinoma cell lines. Cancer Cell Int 2005;5:29.

Hepatology Research 2009; 39: 107–116 doi: 10.1111/j.1872-034X.2008.00441.x

Review Article

Assessment of liver function for safe hepatic resection

Yasuji Seyama and Norihiro Kokudo

Hepato-Biliary-Pancreatic Surgery Division, Department of Surgery, Graduate School of Medicine, University of Tokyo, Tokyo, Japan

The preoperative assessment of liver function is extremely important for preventing postoperative liver failure and mortality after hepatic resection. Liver function tests may be divided into three types; conventional liver function tests, general scores, and quantitative liver function tests. General scores are based on selected clinical symptoms and conventional test results. Child–Turcotte–Pugh score has been the gold standard for four decades, but the Child–Turcotte–Pugh score has difficulty discriminating a good risk from a poor risk in patients with mild to moderate liver dysfunction. The model for end-stage liver disease score has also been applied to predict short-term outcome after hepatectomy, but it is only useful in patients with advanced cirrhosis. Quantitative liver function tests overcome the drawbacks of general scores. The indocyanine green retention rate at 15 minutes (ICG R15) has been reported to be a significant predictor of postoperative liver failure and mortality. The safety limit of the hepatic parenchymal resection rate can be estimated using the ICG R15, and a decision tree (known as the Makuuchi criteria) for selecting patients and hepatectomy procedures has been proposed. Hepatic resection can be performed with a mortality rate of nearly zero using this decision tree. If the future remnant liver volume does not fulfill the Makuuchi criteria, preoperative portal vein embolization should be performed to prevent postoperative liver failure. Galactosyl human serum albumin-diethylenetriamine-pentaacetic acid scintigraphy also provides data that complement the ICG test. Other quantitative liver function tests, however, require further validation and simplification.

Key words: indocyanine green, liver function test, postoperative liver failure, TcGSA

1. INTRODUCTION

THERE ARE MANY causes of liver dysfunction, including viral hepatitis, fatty liver disease, cholestasis, and chemotherapy-associated steatohepatitis. Liver cirrhosis arising from viral hepatitis is a major cause of liver dysfunction in patients with primary liver tumors.[1–4] In patients with metastatic liver tumors, chemotherapy-associated liver dysfunction (including steatosis, steatohepatitis, and sinusoidal injury) has been reported as a risk factor for hepatectomy.[5,6] Postoperative liver failure is a serious complication with a high mortality rate; therefore, the assessment of liver function, which can predict the risk of liver failure and mortality, is absolutely necessary for safe hepatic resection. However, the liver is a multi-functioned organ and a single comprehensive liver function test does not exist.

Correspondence: Dr Norihiro Kokudo, Hepato-Biliary-Pancreatic Surgery Division, Department of Surgery, Graduate School of Medicine, University of Tokyo, 7-3-1 Hongo, Bunkyo-ku, Tokyo 113-8655, Japan. Email: kokudo-2su@h.u-tokyo.ac.jp
Received 5 July 2008; revision 2 August 2008; accepted 5 August 2008.

General scores, including the Child-Turcotte-Pugh (CTP) score,[7,8] the Model for End-Stage Liver Disease (MELD) score,[9,10] and Makuuchi criteria,[3] are useful for estimating integrated liver function. Although these general scores are useful, they do have some drawbacks. Several quantitative liver function tests have been introduced to compensate for these drawbacks of general scores.[11] On the other hand, major hepatectomy is a risk in itself, even for patients with normal liver function, and the safety limit of the hepatic parenchymal resection rate must be considered according to the grade of liver dysfunction that is present.

The goals of hepatic functional assessment in liver surgery are proper patient selection and the prediction of the safety limit of the hepatic parenchymal resection rate. In this review article, we describe the present state of liver function assessments in liver surgery and provide guidance for safe hepatic resection.

2. LIVER FUNCTION TESTS

HEPATIC FUNCTION TESTS can be divided into three types (Table 1): conventional liver function tests, scoring systems that integrate clinical and

Table 1 Liver function tests

1. Conventional tests	
Test	Function/event measured
Serum bilirubin	Uptake, conjugation, excretion
Albumin	Synthesis
Alkaline phospatase	Cholestasis
Gamma-glutamyl transpeptidase	Cholestasis
Transaminases	Necrosis, enzyme induction, alcohol abuse
Coagulation factors: prothrombin time	Synthesis
Serum bile acids	Excretion, shunting
Pletelet count	Portal hypertension
2. General score	
Score	Parameters
Child-Turcotte-Pugh score	serum bilirubin, albumin, PT%, ascites, encephalopathy
MELD score	serum bilirubin, creatinine, and INR
Makuuchi criteria (decision tree)	Ascites, serum bilirubin, ICG R15
3. Quantitative liver function tests	
Tests	Function tested
Aminopyrine breath test	Microsomal function
Antipyrine clearance	Microsomal function
Caffeine clearance	Microsomal function
Lidocaine clearance (MEGX)	Microsomal function
Methacetin breath test	Microsomal function
Galactose elimination capacity (GEC)	Cytosol function
Low-dose galactose clearance	Hepatic perfusion (liver blood flow)
Sorbitol clearance	Hepatic perfusion (liver blood flow)
ICG disappearance	Hepatic perfusion, anion excretion
Albumin synthesis	Synthetic function
Urea synthesis	Synthetic function
99mTc-GSA	Functional hepatocyte mass

laboratory variables, and quantitative liver function tests, the latter of which may theoretically be the most relevant to liver surgery. Conventional liver function tests include well-known and simple, but very important, laboratory parameters. They represent a variety of liver functions, as listed in Table 1; however, none of these parameters provide quantitative information regarding the hepatic functional reserve. Among these tests, the serum total bilirubin, prothrombin time, and serum albumin are integrated in the CTP criteria.

3. GENERAL SCORE

3.1. Child-Turcotte-Pugh score

IN 1964, CHILD and Turcotte proposed a grading system for liver function to predict the outcome of portal hypertensive patients undergoing a port-caval shut.[7] This grading system was later modified by Pugh *et al.* in 1973, and the system has subsequently been known as the CTP score.[8] Five simple parameters were selected based on their experiences: (i) the presence or absence of encephalopathy; (ii) the presence or absence of ascites; (iii) the serum total bilirubin level; (iv) the serum albumin level, (v) and the prothrombin time. The CTP score is a simple system for grading liver function based on these five easily measurable factors and has been considered a gold standard for more than four decades.

The CTP score has also been shown to predict the short-term and long-term outcomes of patients undergoing liver resection. Franco et al. showed that CTP A patients with HCC were good candidates for surgical resection.[2] However, most hepatic dysfunction in surgical candidates is slight or moderate and might not be fully evaluated using the CTP score. A major drawback of the CTP scoring system is the so-called "floor and ceiling effect". Most patients who undergo elective hepatic resection are classified as CTP A, but some risk postoperative liver failure and mortality exists even in this group of patients.[2,4,12–15] The CTP scoring system is not able to discriminate the risk of liver failure in patients with low scores of 5–6 points in class A, that is, the "floor effect". In fact, patients with CTP A are found to have a wide variety of liver functional reserves when assessed using quantitative tests (Fig. 1).[16,17] In other words, we must be able to identify "good-risk" and "poor-risk" CTP A patients to determine the safety margin for liver resection. Quantitative liver function tests are useful for this purpose. On the other hand, patients with CTP C exhibit a wide range of cirrhosis severity, that is, the "ceiling effect". Huo *et al.* proposed a modified CTP scoring system containing a class D to discriminate the severity of cirrhosis.[18]

3.2. The MELD score

Malinchoc *et al.* performed a multivariate analysis to predict the short-term results after transjugular intra-

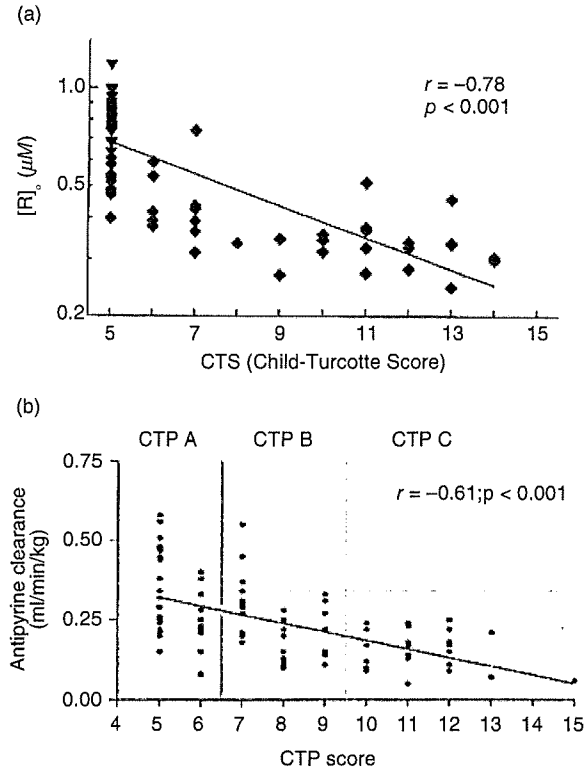

Figure 1 Relationship between Child–Turcotte–Pugh (CTP) score and receptor amount of (a) Galactosyl human serum albumin-diethylenetriamine-pentaacetic acid scintigrams TcGSA and (b) antipyrine clearance. (From Pimstone *et al.* and Mahmoud *et al.*, with permission.)

hepatic portosystemic shunt (TIPS) procedure performed at the Mayo Clinic and reported that the serum concentrations of bilirubin and creatinine, the international normalized ratio for prothrombin time (INR), and the cause of the underlying liver disease were significant predictors of survival and, furthermore, that the Mayo model was superior to CTP classification.[9] This model was slightly modified and is now widely used as the Model for END-Stage Liver Disease (MELD) score; the formula for the MLED score is $3.8*\log_e$(bilirubin [mg/dL]) + 11.2* $\log_e$(INR) + 9.6*$\log_e$(creatinine [mg/dL]) + 6.4*(etiology: 0 if cholestatic or alcoholic, 1 otherwise).[10] The MELD score can be used to predict the mortality risk of patients with end-stage liver disease and is applied for the allocation of donor livers.[10,19] Considering its origin, the MELD score may overcome the drawback of the CTP score's ceiling effect.

The MELD score has also been applied to predict the postoperative mortality risk of patients undergoing hepatic resection. In a study of 82 patients with cirrhosis, 13 of whom died postoperatively, Teh *et al.* reported that a MELD score ≧ 9, the clinical tumor symptoms, and the ASA (American Society of Anesthesiologists) score were independent predictors of mortality after the hepatic resection of hepatocellular carcinoma.[20] Similarly, Cucchetti and colleagues showed that cirrhotic patients with a MELD score equal to or above 11 had a high risk of postoperative liver failure in their report, 11 of 154 cirrhotic patients who underwent a hepatectomy experienced liver failure.[21] Of note, however, the MELD score was not useful for predicting postoperative mortality in patients without cirrhosis.[14,15] Schroeder and coworkers reviewed the records of 587 patients who had undergone elective hepatic resection for primary or metastatic liver tumors or benign diseases and showed that their mean MELD score, which was 6.5 ± 4.5 (SD) was not significantly related to mortality.[14] Instead, they insisted that the CTP and ASA scores were superior for predicting the short-term outcomes. Teh *et al.* performed a case-controlled study of consecutive patients with or without cirrhosis undergoing hepatic resection for hepatocellular carcinoma and reported that the MELD score failed to predict postoperative outcomes in patients without cirrhosis.[15] Presumably, the majority of patients undergoing elective hepatectomy have a low MELD score compared to that of patients undergoing TIPS or liver transplantation. The MELD score may be useful only in patients with advanced cirrhosis. An on-line worksheet for assessing postoperative mortality risk in patients with cirrhosis using age, the ASA score, the serum bilirubin level, the serum creatinine level, the INR, and the etiology of the cirrhosis is available at http://www.mayoclinic.org/meld/mayomodel9.html.

3.3. Makuuchi criteria

A decision tree for hepatectomy procedure has been proposed by Makuuchi *et al.* (Fig. 2).[3] This surgical algorithm is the most popular in Japan and has had a great impact on the improvement of operative mortality and morbidity in hepatoma patients. The decision tree involves only three parameters: the presence or absence of uncontrollable ascites, the serum bilirubin level, and the indocyanine green retention rate at 15 minutes (ICG R15). Patients with uncontrollable ascites and a high bilirubin level are not candidates for hepatic resection. The extent of the hepatectomy procedure is selected according to the ICG R15 value, which appears at the bottom of the decision tree. Because the ICG R15 is not a linear quantitative parameter, only the surgical procedure, and not the exact numbers for the hepatic

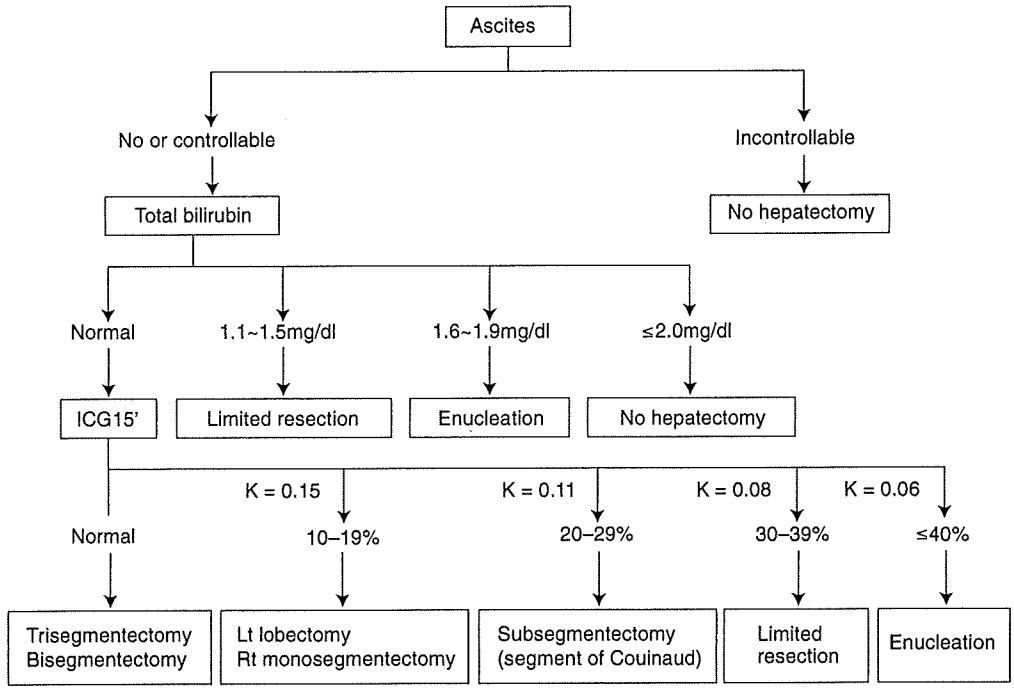

Figure 2 Makuuchi criteria for safe hepatic resection. (From Makuuchi *et al.*, with permission.)

parenchymal resection rate, is presented for each ICG category. For example, a cirrhotic patient with an ICG value of 20% does not have twice the hepatic functional reserve of a patient with an ICG value of 40%. Using this decision tree, hepatic resection can be performed with almost zero mortality.[3,13,22] These results suggest that hepatic resection can be safely performed in patients meeting the Makuuchi criteria, with the extent of the resection based on the ICG R15 value. Thus, the ICG test might be useful for discriminating good and poor risk CTP A patients.

4. QUANTITATIVE LIVER FUNCTION TESTS

A NUMBER OF quantitative liver function tests have been reported to meet the needs of hepatic surgeons. Quantitative liver function tests assess a specific aspect of hepatic function, that is, the liver functions of the microsome, cytosol, anion excretion, urea synthesis, or receptors on the hepatocyte membrane (Table 1).[11] The clearance of intravenously administered exogenous substances that are eliminated or metabolized only by the liver are used for quantitative liver function tests, and the intrinsic clearance and hepatic flow are regards as determinants. The clearance of low extractable substances represents microsomal function (aminopyrine, antipyrine, caffeine, lidocaine, and metatherin) or cytosol function (galactose). On the other, the clearance of high extractable substances, such as sorbitol, low dose galactose, and ICG, represents hepatic flow.[23] Galactosyl human serum albumin-diethylenetriamine-pentaacetic acid scintigrams (TcGSA) measure receptors on the hepatocyte membrane and indicate the functional hepatic mass. Breath tests using an inactive isotope carbon 13, such as ^{13}C-Phenylalanine[21] or ^{13}C-methacetin, have been increasingly used for research purposes.[24,25]

Most of these quantitative function tests, however, have not been shown to be superior to conventional general scores, such as the CTP score, for predicting the surgical outcome of hepatectomy.[26] Furthermore, the methods of quantitative liver functional tests are generally more complex than the ICG clearance test; consequently, these tests tends to be used for clinical research, but not for routine practice. At present, only the ICG test and GSA scintigraphy are widely accepted for clinical use in Japan.

4.1. ICG clearance test

After a bolus injection of indocyanine green, the dye binds to plasma proteins, and is removed exclusively by

the liver through a carrier-mediated mechanism; the dye is ultimately excreted unchanged into the bile. It is not metabolized and does not undergo enterohepatic circulation. The disappearance curve of ICG has two components, a distribution and an elimination phase, and the turning point of these two phases is 20–30 min. ICG has a relatively high intrinsic clearance; therefore ICG retention at 15 minutes (ICG R15) represents hepatic perfusion. ICG R15 most likely increases in patients with cirrhosis because of intrahepatic shunt and sinusoidal capillarization. Intrahepatic shunts decrease the actual hepatic perfusion. Sinusoidal capillarization prevents the free diffusion of protein with high molecular weight such as albumin, and the uptake of ICG-bound protein also decreases. As a result, the clearance of ICG is delayed in patients with cirrhosis, and the extent of the increases in ICG R15 reflects the degree of liver dysfunction. The transportation of ICG competes with that of bilirubin; therefore, the ICG test is not suitable for patients with jaundice.

The ICG test provides additional information to the CTP score, and may overcome the drawbacks of the latter system. The ICG R15 was recommended as grade B for the assessment of liver function before surgery in recently developed evidence-based clinical guidelines for the treatment of hepatocellular carcinoma in Japan.[27] The ICG test is particularly useful as a predictor of postoperative death. Hemming *et al.* reported that ICG clearance was the only test that predicted the risk of liver failure and mortality after hepatic resection and that no other liver function test was useful for this purpose.[12] In a study of 315 patients, Nonami *et al.* found 24 patients with liver failure and showed that the ICG clearance and intraoperative blood loss were significant predictors of postoperative liver failure.[28] Fan *et al.* reported that 101 patients underwent major hepatic resection, with a mortality rate of 13.8%; an ICG R15 value of 14% was the cutoff point for patient short-term survival according to a discriminant analysis.[4] Lau *et al.* reported that 127 patients underwent hepatic resection and 14 patients (11%) died postoperatively; in their study, ICG R15 was the only test that could discriminate between survivors and non-survivors.[26] They presumed that the safety limit was an ICG R15 value of 14% for major hepatectomy and 23% for minor hepatectomy. However, their decision algorism did not include the resection rate of the hepatic parenchymal volume.

The hepatic parenchymal resection rate calculated by computed tomography, that is, the remnant liver volume rate, is another important aspect of preventing postoperative liver failure.[1,29,30] Okamoto *et al.* reported

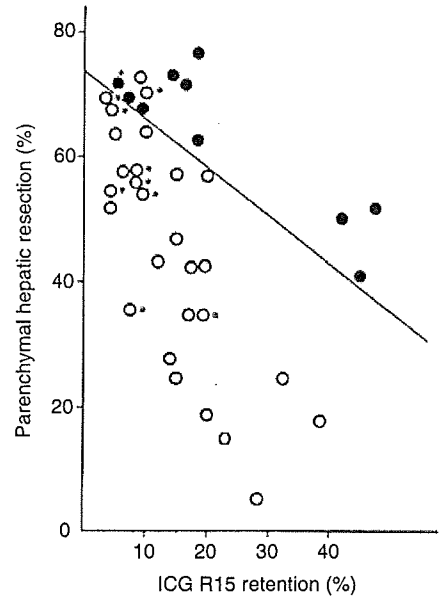

Figure 3 Relationship between indocyanine green retention rate at 15 minutes (ICG R15) and parenchymal hepatic resection rate relative to patient outcome. ○, survivors; ●, non-survivors; ※, patients who did not have cirrhosis ($n = 10$). (From Okamoto *et al.*, with permission.)

a close relationship between the ICG R15 and the parenchymal hepatic resection rate relative to postoperative liver failure in a study of 38 patients, 10 of whom died (Fig. 3).[1] A two-pronged approach using the ICG R15 and the liver resection rate (remnant rate) is extremely important for predicting the surgical risk of liver failure and mortality and to decide on the surgical procedure that should be used to perform a hepatectomy in patients with impaired livers. If the future remnant liver (FRL) volume does not fulfill the Makuuchi criteria, preoperative portal vein embolization (PVE) should be performed to prevent postoperative liver failure as mentioned later.[29,31,32]

4.2. TcGSA scintigram

The asialoglycoprotein (ASGP) receptor is a hepatic cell surface receptor observed only in mammals. Intravenously administered TcGSA (galactosyl human serum albumin -diethylenetriamine- pentaacetic acid) rapidly binds to the asialoglycoprotein receptor and is taken up by the hepatocytes.[33] A typical time activity curve after the injection of TcGSA in healthy subjects is shown in Figure 4.[34] The characteristics of TcGSA are as follows: (i) GSA is taken up only by the liver; (ii) accumulation in

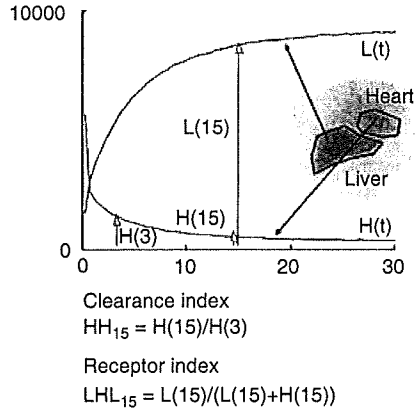

Figure 4 HH15 and LHL15. The clearance index HH15 and the receptor index LHL15 are calculated from three points of data in the time activity curves. (From Torizuka *et al.*, with permission.)

the liver is rapid; (iii) not only blood clearance, but also hepatic uptake of GSA can be estimated; (iv) continuous time activity data can be obtained; and (v) the ligand-receptor binding is a second-order process. In other words, we can safely inject an amount of GSA that will occupy a significant fraction of the receptor.

The clearance index HH15 (heart 15/heart 3) and the receptor index LHL15 (liver 15/heart 15 + liver 15) are simple indicators calculated from three points of data in the time activity curves (Fig. 4).[34] The LHL15 has been reported to be associated with ICG R15 and postoperative complications.[35] To be precise, HH15 and LHL15 are not indices of total functional hepatocyte mass; therefore, R_0 (receptor amount),[36] R_{max} (maximal removal rate of ASGP),[37] R_{total} (total ASGP receptor amount),[38] $R_{0\text{-remnant}}$ (total amount of the remnant liver),[39] and GSA-RL (R_{max} in the future remnant liver)[40] are calculated using a kinetic model and are used as quantitative parameters. TcGSA scintigrams have a history of being used for 17 years but have become popular in only the last 10 years, and the modality is now known in Japan as a useful parameter, in addition to ICG R15, for predicting the outcome of hepatic resection.[27,41] As the $R_{0\text{-remnant}}$ and GSA-RL represent the functional reserve after hepatectomy, these parameters may be superior to ICG R15 for predicting postoperative liver failure.[40,42] Kokudo *et al.* reported a close relationship between the amount of receptors in the remnant liver and postoperative liver failure (Fig. 5).[42]

Because of the above-mentioned excellent short-term outcomes after hepatic resection when performed according to the ICG R15 value, new liver function tests, including TcGSA scintigrams, are now used only for patients whose liver function cannot be fully estimated using an ICG based algorithm, such as patients with jaundice or ICG intolerance.

4.3. Galactose elimination capacity

Galactose is a high extractable substance after low dose administration, and its clearance represents hepatic flow. However, galactose is a harmless substance and is unique because it can be administered as a saturating dose. Galactose elimination capacity (GEC) is determined by serial measurement of serum concentration after administration of saturating dose of galactose (0.5mg/kg), and represents cytosolic metabolic capacity of the liver.[11] GEC has been used to determine functional reserve of the severe liver disease, such as fulminant liver failure, primary biliary cirrhosis, or chronic active hepatitis. Recently, Redaelli *et al.* reported that preoperative GEC predicted the complications and

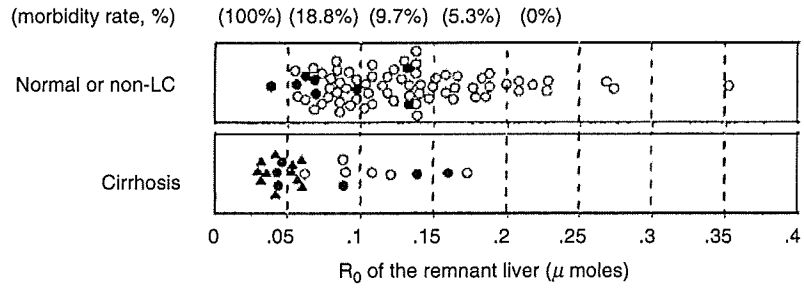

Figure 5 Relation between receptor amount in the remnant liver and postoperative liver failure. The close and open circles indicate patients with and those without complications indicating liver failure, respectively. The morbidity rate in patients with a remnant receptor amount of less than 0.05 μmoles was 100% and the rate decreased in inverse proportion to the remnant receptor amount. (From Kwon *et al.*, with permission.)

mortality after hepatic resection.[43] In the study of 258 patients with liver resection, 78 for HCC and 180 for non-HCC, GEC less than 4 mg/min/kg and 6 mg/min/kg was significantly associated with postoperative complications and death in patients with HCC and non HCC, respectively. GEC has been used to measure liver cytosolic liver function after in donors and recipients of living donor liver transplantation.[44] The drawback of GEC is that it is of no value in detecting minor functional impairment. GEC has possibility to complement the CTP score and ICG R15, but a strategy of safe hepatic resection based on GEC has not yet been described. To determine the safety limit for hepatic resection rate in relation to the GEC is a future issue.

5. SELECTION OF HEPATECTOMY PROCEDURE

THE MORTALITY RATE after hepatic resection has been improved thanks to advances in liver surgery and is now reported to be less than 5% in high-volume centers.[45–47] Patient selection is usually made based on the CTP score. In principle, patients with CTP A are candidates for hepatic resection in western countries. Furthermore, a Barcelona group insisted that portal pressure evaluated using the hepatic venous pressure gradient (HVPG) was the only significant predictive factor of postoperative hepatic decompensation and that hepatectomies should be restricted to patients with portal hypertension.[48] Portal hypertension has been adopted by the Barcelona Clinic Liver Cancer (BCLC) staging classification, in which the treatment schedule is determined according to both tumor progression and liver function.[49]

In Japan and other Eastern countries, the ICG test is routinely performed in addition to the CTP score, although the ICG test is not as popular in western countries. Patients with CTP A and some patients with CTP B are considered candidates for hepatectomy. The safety limit of the hepatectomy procedure is determined using ICG-based criteria, such as the Makuuchi decision tree, and this method has become a gold standard, in addition to the CTP score, in Japan. As a result, the average mortality rate after hepatectomy was 0.9% in Japan according to a nation-wide study,[50] and zero mortality among 1056 consecutive patients over an 8-years period has been reported by our institution.[13] Evidence-based clinical guidelines have proposed an algorithm for the treatment of HCC, which is determined according to the degree of liver damage and the tumor status.[27] The degree of liver damage is classified as class A, B, and C using the presence of ascites, the serum total bilirubin, the serum albumin, the ICG R15, and the prothrombin time,[51] and patients with class A or B are recommended to undergo resection if the number of tumors is less than three.[27]

ICG R15 was shown to be a significant predictor of liver failure and mortality after hepatectomy in the 1980s and early 1990s when the mortality rate was over 10%. The safety limit for the hepatic resection rate in relation to the ICG R15 had been estimated. Recently, 3D virtual hepatectomy simulation based on liver circulation has been developed, and the liver resection volume of planned hepatectomy can be more precisely predicted.[52,53] The safety limit for hepatic resection rate may be reevaluated using the new approach in the future. In the era of nearly zero mortality, prospective studies of new assessments of hepatic function are difficult to plan using mortality after hepatectomy as an endpoint. New liver function tests must instead be more convenient and precise than the CTP score, the ICG test, or the TcGSA scintigrams.

The risk of liver dysfunction as a result of chemotherapy, that is, steatosis, steatohepatitis, and sinusoidal obstructive syndrome, has been described in patients who have received chemotherapy for colorectal cancer and liver metastasis, and microscopic findings in background liver tissue from resected specimens are related to surgical outcome after hepatic resection.[5,6,54] However, the preoperative assessment of liver function after neo-adjuvant chemotherapy has not yet been established.

6. INDICATION FOR PORTAL VEIN EMBOLIZATION

IN ADDITION TO liver function tests, the remnant liver volume is another important aspect of safe hepatic resection.[30,55] If FRL volume is not enough to perform hepatectomy safely, indication of PVE should be considered.[31,32] Originally, PVE was indicated if the rate of FRL volume was fewer than 40% in the patients with normal liver, and fewer than 50% in those with injured liver, i.e. with an ICG R15 value between 10–20% or with jaundice.[29,31] These extensions of indication of major hepatic resection have been proved useful for both patients with hilar cholangiocarcinoma and with hepatocellular carcinoma.[56,57] On the other hand, Vauthy *et al.* described the indication of PVE as followings: PVE was indicated when the FRL volume was ≤ 20% of the estimated total liver volume in patients with normal liver, ≤ 30% in patients with